

# SAMD12 as a Master Regulator of MAP4Ks by Decoupling Kinases From the CNKSR2 Scaffold

Wen Pan <sup>1</sup>, Zhijie Lin <sup>2</sup>, Shiwen Chen <sup>1,3</sup>, Jiahui Li <sup>4</sup>, Yu Wang <sup>1</sup>, Keyu Chen <sup>4,\*</sup>, and Mingjie Zhang <sup>1,4,\*</sup>

- 1 Shenzhen Key Laboratory of Biomolecular Assembling and Regulation, School of Life Sciences, Southern University of Science and Technology, Shenzhen 518055, China
- 2 Zhejiang Key Laboratory of Organ Development and Regeneration, College of Life and Environmental Sciences, Hangzhou Normal University, Hangzhou 311121, China
- 3 Division of Life Science, Hong Kong University of Science and Technology, Clear Water Bay, Kowloon, Hong Kong, China
- 4 Greater Bay Biomedical Innocenter, Shenzhen Bay Laboratory, Shenzhen 518107, China

Correspondence to Keyu Chen and Mingjie Zhang: Greater Bay Biomedical Innocenter, Shenzhen Bay Laboratory, Shenzhen 518107, China. chenky@szbl.ac.cn (K. Chen), zhangmj@sustech.edu.cn (M. Zhang) https://doi.org/10.1016/j.jmb.2025.169034

Editor: M.F. Summers

#### Abstract

The MAP4K member TNIK and the multi-domain scaffold protein CNKSR2, both of which are clustered at neuronal synapses, interact with each other and are closely associated with neurodevelopmental disorders, although the mechanism underlying their interaction is unclear. In this study, we characterized the interaction mechanisms between MAP4K kinases (MAP4K4, MINK1 and TNIK) and the CNKSR1/2/3 scaffold proteins, and discovered that SAMD12, a familial adult myoclonic epilepsy disease gene product, or its close homolog SAMD10, binds to CNKSR1/2/3 with exceptionally strong affinities and can quantitatively displace MAP4K from CNKSR1/2/3 scaffolds. Additionally, we demonstrated that CNKSR2 acts as both a scaffold and an activator of TNIK during neuronal synapse development. Ectopic expression of SAMD12 can effectively alter synapse development, likely by inhibiting TNIK activity through the dissociation of the kinase from CNKSR2. Our findings may have broad implications on the roles of MAP4Ks and CNKSR1/2/3 in the nervous system and in other tissues under physiological and pathophysiological processes.

© 2025 Elsevier Ltd. All rights are reserved, including those for text and data mining, Al training, and similar technologies.

#### Introduction

TNIK (TRAF2 and NCK-Interacting Kinase), a MAP4K family member serine/threonine kinase, exhibits a broad distribution across various tissues including the brain. It plays critical roles in cell migration, cytoskeletal organization, cell proliferation, and metabolism. <sup>1–8</sup> In neurons, TNIK acts as a signaling hub governing diverse neuronal functions such as neuronal migration, axon guidance, dendrite development, synapse formation and function. <sup>9–19</sup> Loss of TNIK protein is causative

of intellectual developmental disorders in patients<sup>20</sup> and in a mouse model.<sup>21</sup> A number of TNIK variants have been linked to psychiatric and neuronal developmental disorders.<sup>22–24</sup> MAP4K4 and MINK1 are two paralogs of TNIK in mammals. These three MAP4Ks share similar sequences and domain organizations and play critical roles in regulating MAP kinase signaling cascades in diverse tissues.<sup>25–27</sup> In addition to nervous system disorders, mutations of these three MAP4Ks are intimately linked to other diseases including various forms of cancers, immune disorders, metabolic diseases,

etc..<sup>27–30,5,6</sup> Despite of the importance of these three MAP4Ks, how their kinase activities and subcellular locations are regulated remain elusive.

TNIK is concentrated in the post-synaptic compartments of neurons, 15 which relies on its interaction with a membrane binding scaffold protein CNKSR2 (connector enhancer of kinase suppressor of Ras 2),19 though with an unclear molecular mechanism. CNKSR2, also known as CNK2 or MAGUIN, is a multidomain scaffold protein highly clustered in dendritic spines capable of binding to a multitude of synaptic proteins including TNIK, PSD-95, LRRC7, and s-Afadin.1 CNKSR2 is implicated in several signaling pathways through its interactions with various binding partners, such as KSR/MEK in MAPK signaling,3 ARHGAP39 in Rho signaling, 37 TNIK in JNK signaling<sup>19</sup> and Cytohesin in Arf signaling.<sup>38</sup> CNKSR2 is known to be important for dendritic development and spine formation. 37 CNKSR2 is one of the causative genes for nonsyndromic X-linked intellectual disability accompanied by epilepsy and aphasia. 39-43 CNKSR2 knockout (KO) mice display increased neural activity and spontaneous electrographic seizures as well as increased anxiety, defects in learning and memory, and a progressive loss of ultrasonic vocalizations, resembling symptoms of Epilepsy-Aphasia Spectrum (EAS) patients.44 In addition, CNKSR2 or its ortholog CNK, has been identified as a RAF-binding molecule involved in RAS signaling in organisms such as drosophila 45-47, worms 48 and humans. 30

Epilepsy ranks among the most prevalent disorders. hallmarked neurological spontaneous and recurrent seizures. Familial Adult Myoclonic Epilepsy (FAME) constitutes an autosomal dominant condition marked intellectual disability and a deterioration in both tremor and myoclonus. 49 Pentameric repeat expansions, involving a concatenation of pathogenic TTTCA repeats in conjunction with TTTTA repeats, have been identified as the etiological agents responsible for nearly all FAME occurrences worldwide. These expansions are found within six distinct SAMD12,50 genes, including RAPGEF2,50 TNRC6A.50 MARCH6,51 YEATS2,52 STARD7,53 all of which are situated within introns of these genes. The mechanisms underlying these pentanucleotide repeat diseases are enigmatic. SAMD12 encodes an evolutionally conserved, small SAM domain containing protein (Figure 1A). Although it is one of the first identified repeat expansion gene causing FAME,<sup>50</sup> functions of SAMD12, or its homolog SAMD10, are poorly explored, except for one recent study indicating that SAMD12 regulates cancer cell motility by binding to CNKSR2.54 The drosophila ortholog of SAMD12/ SAMD10, known as HYP (also referred to as Aveugle or AVE), plays a role in Raf kinase activation by forming a complex with drosophila CNK, thereby promoting KSR-MEK interaction and regulating the MAP kinase signaling pathway in flies. 35,55,56

In this study, we elucidated the molecular mechanism underlying the interaction between CNKSR2 and TNIK or SAMD12. We discover that exceptionally strong SAMD12-CNKSR2 interaction can effectively regulate the TNIK-CNKSR2 interaction, thereby modulating TNIK function in synapses. Our study provides a molecular explanation to why SAMD12 may be involved in neuronal disorders and how the interplay among CNKSR2, TNIK and SAMD12 may modulate neuronal developments and synaptic signaling. Our systematic studies further showed that the mechanisms governing the interactions of CNKSR2 with TNIK and with SAMD12 are conserved for the bindings of the CNKSR family proteins (CNKSR1, CNKSR2 and CNKSR3) to the three MAP4Ks (TNIK, MINK1 and MAP4K4) and to SAMD12/SAMD10.

#### Results

### The CNK family proteins interact with SAMDs and MAP4Ks

The CNK family proteins are evolutionarily conserved scaffold proteins. Three CNK paralogs, CNKSR1, CNKSR2 and CNKSR3, are expressed in mammals. CNKSR1/2/3 have the same domain organization in the N-termini (termed as "CNK-NT" in short): a Sterile Alpha Motif (SAM) domain, a Conserved Region in CNK (CRIC) domain, a PSD-95/DIg-A/ZO-1 (PDZ) domain and a Prolinerich motif (Figure 1A).<sup>57</sup> Since CNKSR2 is specifically expressed in neural tissues, we performed affinity purification coupled with mass spectrometry (AP-MS) using purified StrepII-tagged CNKSR2-NT as the bait to identify its binding proteins from mouse brain lysates. Three MAP4Ks, including TNIK (MAP4K7), MINK1 (MAP4K6) and MAP4K4. as well as SAMD12 were recovered with high confidence in the affinity purification (Figure 1B).

SAMD12 and SAMD10 are orthologs of drosophila HYP, which has been reported to bind Drosophila CNK. 55 To test whether such interaction is conserved in mammalian cells, recombinant SAMD12 and CNKSR2-NT proteins were purified and their binding affinity was determined by Isothermal titration calorimetry (ITC). SAMD12 binds to CNKSR2-NT with very high а (Kd  $\sim$  30 nM) and with a 1:1 stoichiometry (Figure 1C1 and D). Size-exclusion chromatography coupled with multi-angle light scattering (SEC-MALS) experiments further showed that the two proteins formed a stable heterodimer in solution (Figure 1E and F).

ITC-based assays showed that all three paralogs of CNK bind to SAMD12 with nanomolar affinities, with CNKSR1-NT showing the strongest binding

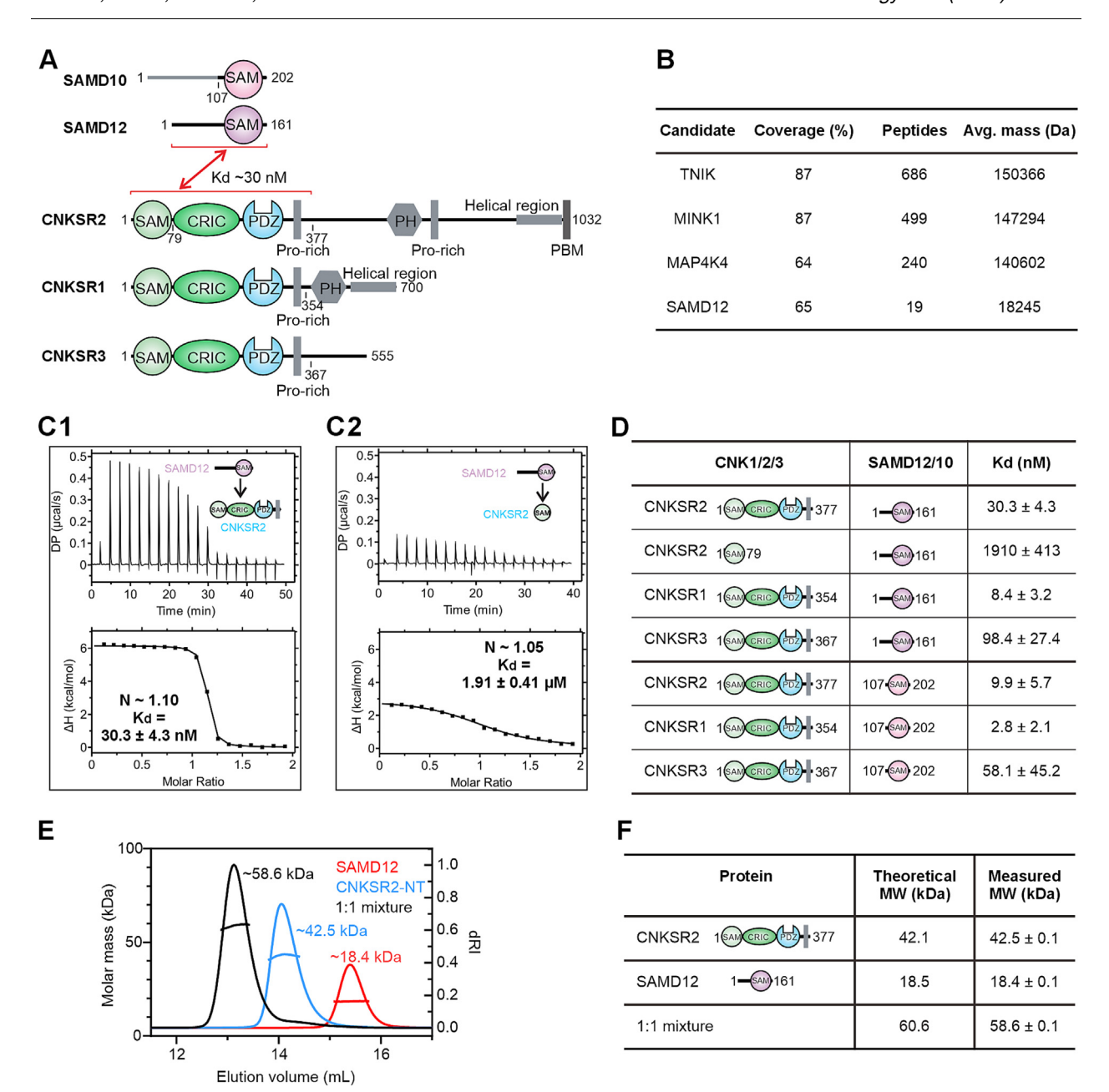
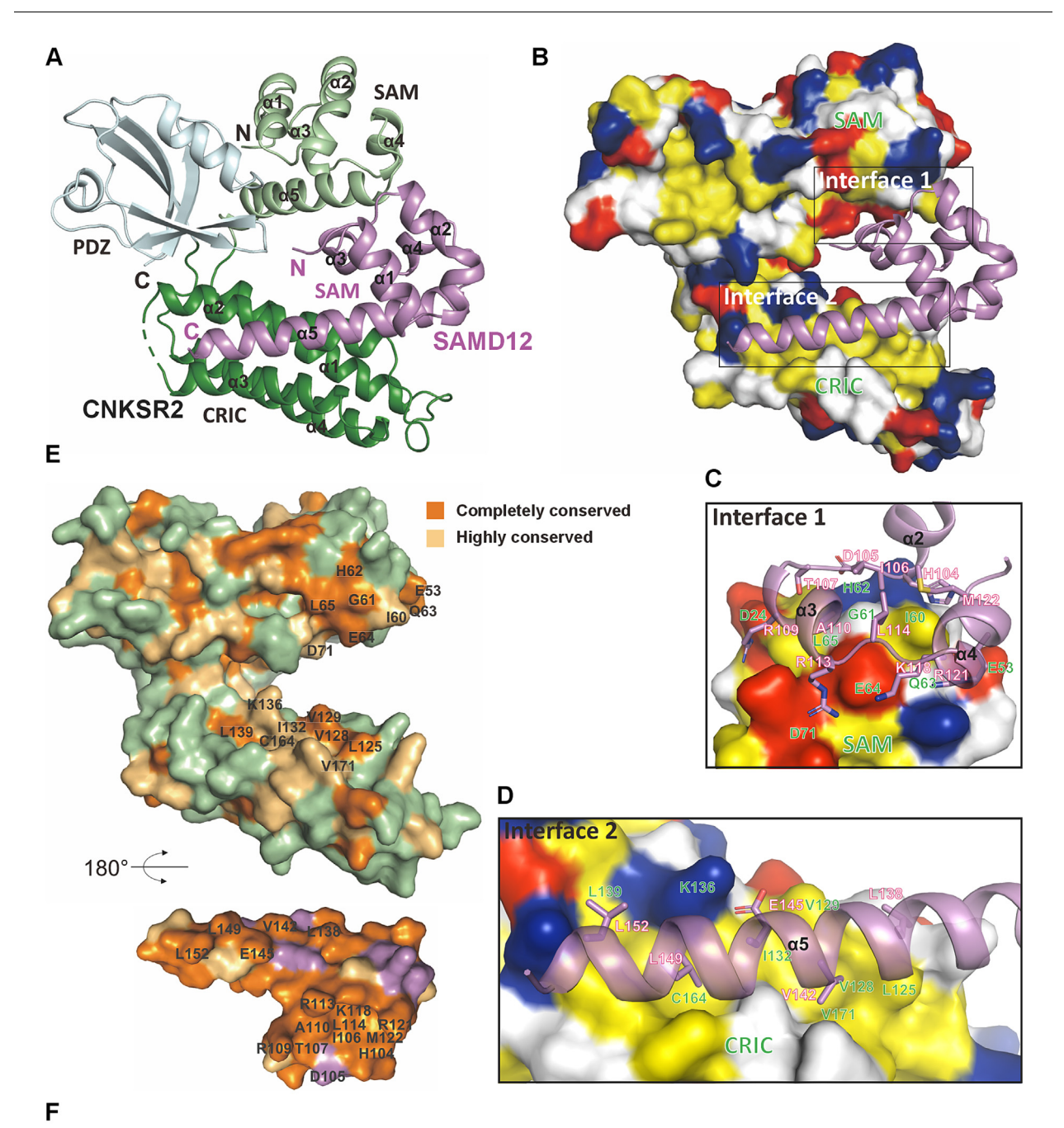


Figure 1. The CNKSR family proteins interact with SAMDs and MAP4Ks. (A) Schematic diagram showing the domain organizations of mouse SAMD10/12 and CNKSR1/2/3. The two-way arrowed line indicates the specific interaction regions between the two families' proteins. (B) Recovered binding proteins of StrepII-tagged CNKSR2-NT from the AP-MS experiments. (C) Isothermal titration calorimetry (ITC) binding curves between CNKSR2-NT and SAMD12 (C1) and between CNKSR2-SAM and SAMD12 (C2). (D) Summarized binding affinities measured by ITC between different CNK family members and SAMD10/12 proteins. (E and F) Size-exclusion chromatography coupled with multi-angle light scattering (SEC-MALS) analysis (E) of CNKSR2-NT (blue line), SAMD12 (red line), and CNKSR2-NT/SAMD12 complex (black line). The theoretical and measured molecular weight are listed in (F).

affinity to SAMD12 with a Kd  $\sim$  8 nM (Figure 1D). Further experiments using truncated CNKSR2 discovered that the SAM domain of CNKSR2 alone can bind to SAMD12 but with a  $\sim$ 60-fold weaker affinity (Kd  $\sim$  1.9  $\mu$ M, Figure 1C1 vs C2), indicating that other regions in CNKSR2-NT (e.g.,

the CRIC domain and/or the PDZ domain) also contribute to the strong interaction with SAMD12. Our ITC-based experiments further showed that, in comparison to SAMD12, SAMD10 binds to each of the CNK proteins with a  $\sim$ 2–3 folds higher affinity (Figure 1D).



SAMD12	CNKSR2-NT	Kd (nM)	Notes	Weakening folds
WT	WT	30.3 ± 4.3		
R121E	WT	302 ± 162	Interface 1	~10
R113E	WT	2070 ± 330	Interface 1	~68
V142Q & L149Q	WT	372 ± 81	Interface 2	~12
R113E & V142Q & L149Q	WT	n.d.	Interface 1 + 2	∞
WT	160Q	74.1 ± 26.3	Interface 1	~2.4
WT	E68R	49.2 ± 11.0	Interface 1	~1.6

## The CRIC and SAM domains of CNKSR2 simultaneously engage with SAMD12 to form a highly stable complex

To delineate the molecular mechanism governing the strong interaction between CNKSR2-NT and the SAM domain of SAMD12, we determined the crystal structure of the CNKSR2-NT in complex with the SAM domain of SAMD12 at the resolution of 2.85 Å (Figure 2A, Table S1). In the complex, the SAM-CRIC-PDZ tandem of CNKSR2-NT assumes a jaw-shaped conformation with the SAM domain and CRIC domain as the upper and lower jaw coordinated by the PDZ domain (with its target binding groove fully accessible), and the jaw "bites" two distinct surfaces of the SAMD12 SAM domain (Figure 2A and B). The first contact surface of the complex involves the characteristic head-to-tail SAM/SAM domain interaction between CNKSR2 SAM and SMAD12 SAM, in which negatively charged residues at the N-terminus of the CNKSR2-SAM α5 helix engage in electrostatic interactions with positively charged residues from the  $\alpha 2/\alpha 3$ - and  $\alpha 3/\alpha 4$ -loops of SAMD12 (Figure 2B and C).58 The second surface is formed by binding of the α5-helix of SAMD12 to the four-helix bundle of the CNKSR2 CRIC domain (Figure 2B and D). The bidentate bindings of the CNKSR2 SAM and CRIC domains to the SAMD12 SAM domain explains the exceptional high binding affinity between the two proteins and rationalizes why the canonical SAM-SAM interaction only has a Kd of  $\sim$ 2  $\mu$ M (Figure 1C). Additionally, the residues involved in the complex formation are extremely conserved in both the CNKSR family proteins and in SAMD12/SAMD10 (Figures 2E, F and S1).

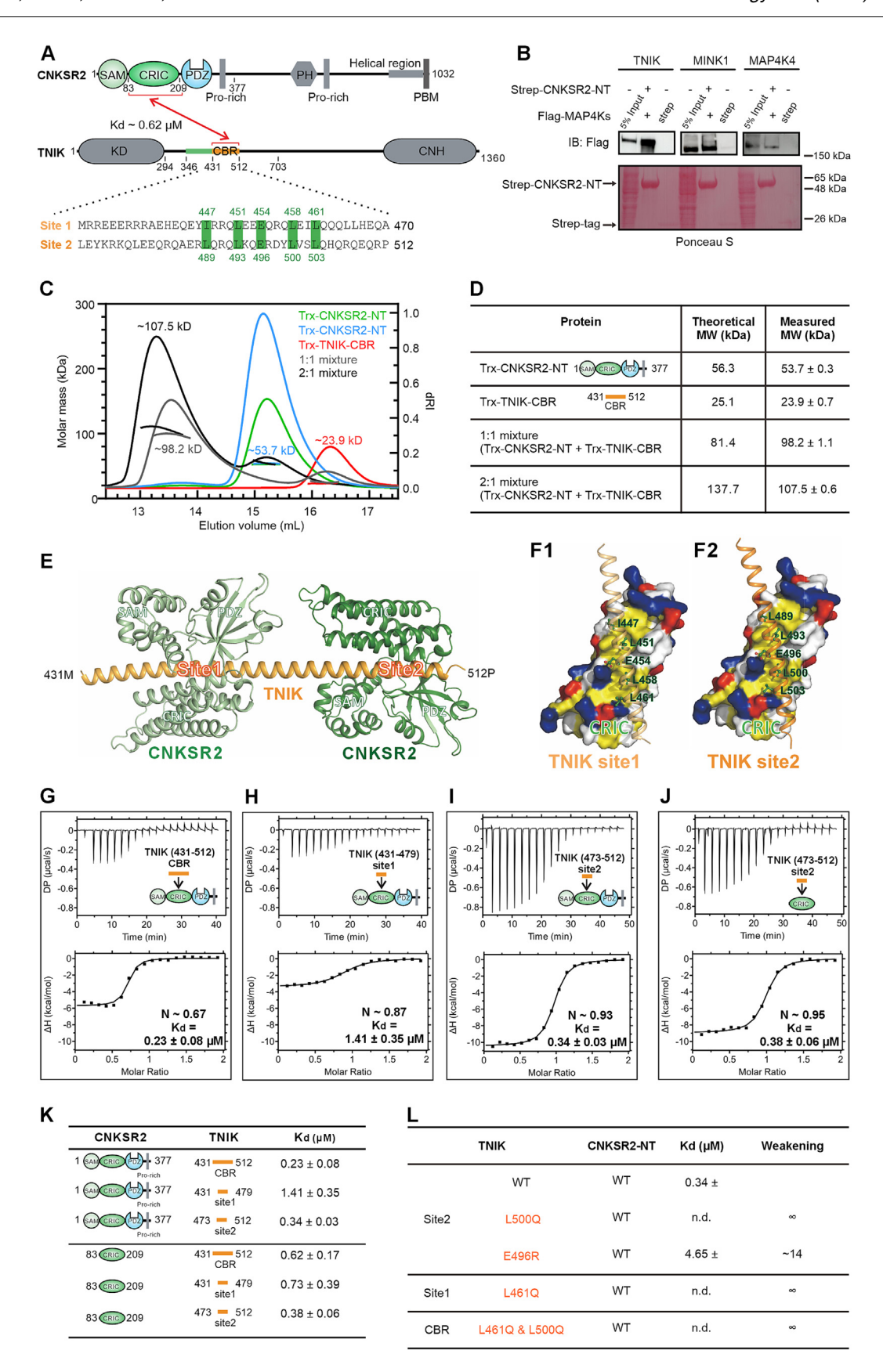
To verify the structural model, we introduced point mutations at the key position on both interfaces (Figure 2F, see Figure S2 for the raw ITC data). At interface 1, the side chains of R113 and K118 in SAMD12 participate in salt bridges with E64 in the SAM domain of CNKSR2. Substitution of R113 with Glu weakened SAMD12's binding to CNKSR2 by approximately ~68-fold (Figure 2C and 2F). R121 of SAMD12 forms hydrogen bonds

with the sidechain of Q63 in CNKSR2 SAM (Figure 2C). Substitution of R121 with Glu also resulted in a  $\sim$ 10-fold reduction in SAMD12's binding to CNKSR2 (Figure 2F). The sidechain of I60 of CNKSR2-SAM packs on the hydrophobic surface formed by I106, L114 and M122 from SAMD12 (Figure 2C), its replacement with a polar Gln reduced binding by  $\sim$ 2-fold (Figure 2F). V142 and L149 of SAMD12 insert into the hydrophobic pocket formed by the CRIC domain of CNKSR2 (Figure 2D), substitutions of both residues with polar Gln led to an  $\sim$ 12-fold decrease in the binding affinity (Figure 2F).

#### TNIK specifically binds to CNKSR2 with a submicromolar affinity

Our affinity purification with CNK-NT as the bait also captured three MAP4Ks as CNKSR2 associated proteins (Figure 1B). MAP4Ks share conserved domain architectures by comprising an N-terminal kinase domain, a middle linker domain with various lengths, and a C-terminal citron homology (CNH) domain (Figures 3A and S3A). Corroborating the AP-MS results, purified Streptagged CNKSR2-NT protein could pull down all Flag-tagged full-length expressed in heterologous cells (Figure 3B). TNIK is highly expressed in neuronal synapses and has been reported to associate with CNKSR2 in synapse, 15,19 although it is not known whether the two proteins directly bind to each other. We chose TNIK as a representative of the MAP4Ks to characterize their interactions with CNKSR2. We split TNIK into two halves in the middle of the linker domain (designated as "TNIK-NT" and "TNIK-CT", see Figure S3 for the detailed sequence boundaries). The subsequent pull-down assay indicated that the binding site is localized within the TNIK-NT half. Further mapping experiments revealed that a helical segment within TNIK-NT (amino acids [aa] 346-512) is both necessary and sufficient for binding to CNKSR2 (Figure S3). It is further noted that this helical segment is unique to MAP4K4, MINK1 and TNIK among all MAP4Ks, explaining why the

Figure 2. Structural basis of the tight binding between CNKSR2 and SAMD12. (A) Ribbon diagram of the CNKSR2-NT/SAMD12-SAM complex structure. The disordered loop between α2 and α3 helices in the CRIC domain is drawn as a dashed line. (B) Combined surface and ribbon representation showing the overall binding interfaces of CNKSR2-NT and SAMD12. In the surface model, hydrophobic, hydrophilic, positively charged and negatively charged residues are colored in yellow, white, blue and red respectively. (C) Combined surface and ribbon-stick representation showing the electrostatic interactions in the Interface 1. (D) Combined surface and ribbon-stick representation showing the hydrophobic interactions in the Interface 2. (E) The amino acid conservation map of residues in the two interfaces of the CNKSR2/SAMD12 complex. Residues that are completely and highly conserved in all members of CNKSRs or SAMDs are shown in brown and light brown respectively, and non-conserved residues are in pale green and purple for CNKSRs and SAMDs, respectively. The detailed amino acid sequence alignments used to construct the figure are shown in Figure S1. (F) ITC-based measurements comparing the binding affinities between SAMD12 (WT or mutants) and CNKSR2-NT (WT or mutants). "n.d." denotes not detectable.



CNKSR family proteins selectively bind to these three MAP4Ks (Figure S3).

To unravel the interaction details, the CNKSR2 binding region on TNIK was further mapped to aa 346-512, termed as CBR (Figures 3A and S3). In SEC-MALS experiments, we noticed that isolated CNKSR2-NT and TNIK-CBR were each eluted as a monomer. Up to two molecules of CNKSR2-NT can bind to each copy of TNIK-CBR (Figure 3C and D). Consistently, ITC-based assays showed that CNKSR2-NT binds to CBR with an apparent Kd  $\sim$  0.23  $\mu$ M and an N number significantly small than 1 (Figure 3G and K). These observations indicate that CNKSR2 bind TNIK in a 2:1 ratio. Unfortunately, crystallization of the CNKSR2-NT/ TNIK-CBR complex in 1:1 or 2:1 ratio failed to generate crystals, so we turned to AlphaFold3<sup>59</sup> to predict the binding model between CNKSR2-NT and the TNIK helical segment (aa 346-512). Among the top ranked predicted complex structures, CNKSR2-NT binds to one of the two consecutive sites (Site 1 and Site 2) in the helical region spanning residues 431-512 (CBR) (Figure 3A and E). Only the CRIC domain of CNKSR2 is involved in binding to the TNIK helix, and the two short helices (Site 1 and Site 2) bind to the CNKSR2 CRIC domain with an essentially same binding mode (Figure 3E and F). When CNKSR2-NT were modeled to simultaneously bind to both sites on TNIK-CBR (aa 431-512) based on predicted structures, the two molecules CNKSR2-NT can occupy both sites without any steric restrictions (Figure 3E), indicating each TNIK can bind to two copies of CNKSR2. Amino acid sequence analysis revealed that the key residues in the two TNIK sites responsible for binding to the CNKSR2 CRIC domain can be nicely aligned with each other (Figure 3A). In line with the predicted structure model, ITC-based assays showed that CNKSR2-NT binds to TNIK-Site1 with a Kd  $\sim$  1.41  $\mu\text{M}$  and an N number near 1 (Figure 3H and K), and to Site2 with a few-fold higher affinity (Kd  $\sim$  0.34  $\mu$  M) and also with an N number near 1 (Figure 3I and K). The above structural and biochemical analysis conclusively demonstrates that CNKSR2-NT can simultaneously and independently bind to two sites in the helical segment of TNIK. Finally, we showed that the CRIC domain of CNKSR2 is sufficient in binding to the helical segment of TNIK as the CNKSR2 CRIC domain and CNKSR2-NT bind to each site with essentially same affinities (see Figure 3I vs J to show the bindings to Site2 as an example).

The predicted model suggests that TNIK's Site1 Site2 utilize a highly similar binding and interact CNKSR2, with mechanism to characterized by the insertion of their hydrophobic residues into a hydrophobic groove of the CRIC domain (Figure 3F). Consistent with the modeled structure, substitution of a hydrophobic residue L500 with a polar Gln obliterated the interaction between TNIK-site2 and CNKSR2-NT (Figure 3F2 and L). Apart from hydrophobic interactions, charge-charge interaction mediated by E496 in TNIK and K136 in CNKSR2 are also predicted to contribute to the CNKSR2/TNIK interaction (Figure 3F2). The charge-reversing mutation E496R in TNIK-CBR Site2 diminished the binding by approximately 14-fold (Figure 3F2 and L). Correspondingly, substitution of L461 in Site1 binding disrupted this site's to CNK-NT (Figure 3L). The L461 and L500 double mutant of TNIK-CBR or the full-length TNIK (abbreviated as "TNIK-mutant") exhibited no detectable binding to CNKSR2 (Figure 3L). This CNKSR2 binding

Figure 3. TNIK-CBR binds to CNKSR2-CRIC with sub-micromolar affinities. (A) Schematic diagram showing the domain organizations of CNKSR2 and TNIK. The rectangle represents predicted helical region in the middle of TNIK, and CBR (CNK-binding region) is colored in orange. The two-way arrowed line illustrates the interaction regions within these two proteins. The amino acid sequences of Site 1 and Site 2 in the CBR of TNIK are aligned. The key residues responsible for CNK-binding are highlighted by green background. (B) Pull-down assay showing the interactions between CNKSR2-NT and full-length MAP4Ks. StrepII tagged recombinant CNKSR2-NT protein was mixed with HEK293T cell lysates, which were transfected with full-length Flag-TNIK. Flag-MINK1 or Flag-MAP4K4. and then pulled-down by Strep-Tactin beads. (C and D) The SEC-MALS analysis (C) of CNKSR2-NT (green and blue line), TNIK-CBR (red line), and the CNKSR2-NT/TNIK-CBR complex (gray and black line). The theoretical and measured molecular weights are listed in (D). (E) A structure model of the TNIK-CBR and CNKSR2-NT complex predicted by AlphaFold3 shows a 1:2 stoichiometry binding. (F) Combined surface and ribbon-stick representation showing the interactions between CNKSR2-CRIC and TNIK-site1 (F1) and TNIK-site2 (F2) from the predicted complex structure. Residues of the CRIC-binding motif are labelled in green. (G-J) Representative ITC curves showing sub-micromolar binding affinities between TNIK and CNKSR2. TNIK-CBR binding to CNKSR2-NT (G), TNIKsite1 binding to CNKSR2-NT (H), TNIK-site2 binding to CNKSR2-NT (I), and TNIK-site2 binding to CNKSR2-CRIC CNKSR2-NT (J). (K) Summary of the affinities determined by ITC describing the bindings between different CNKSR2 constructs and TNIK variants. (L) ITC-based measurements comparing the binding affinities between TNIK (WT or mutants) and CNKSR2-NT.

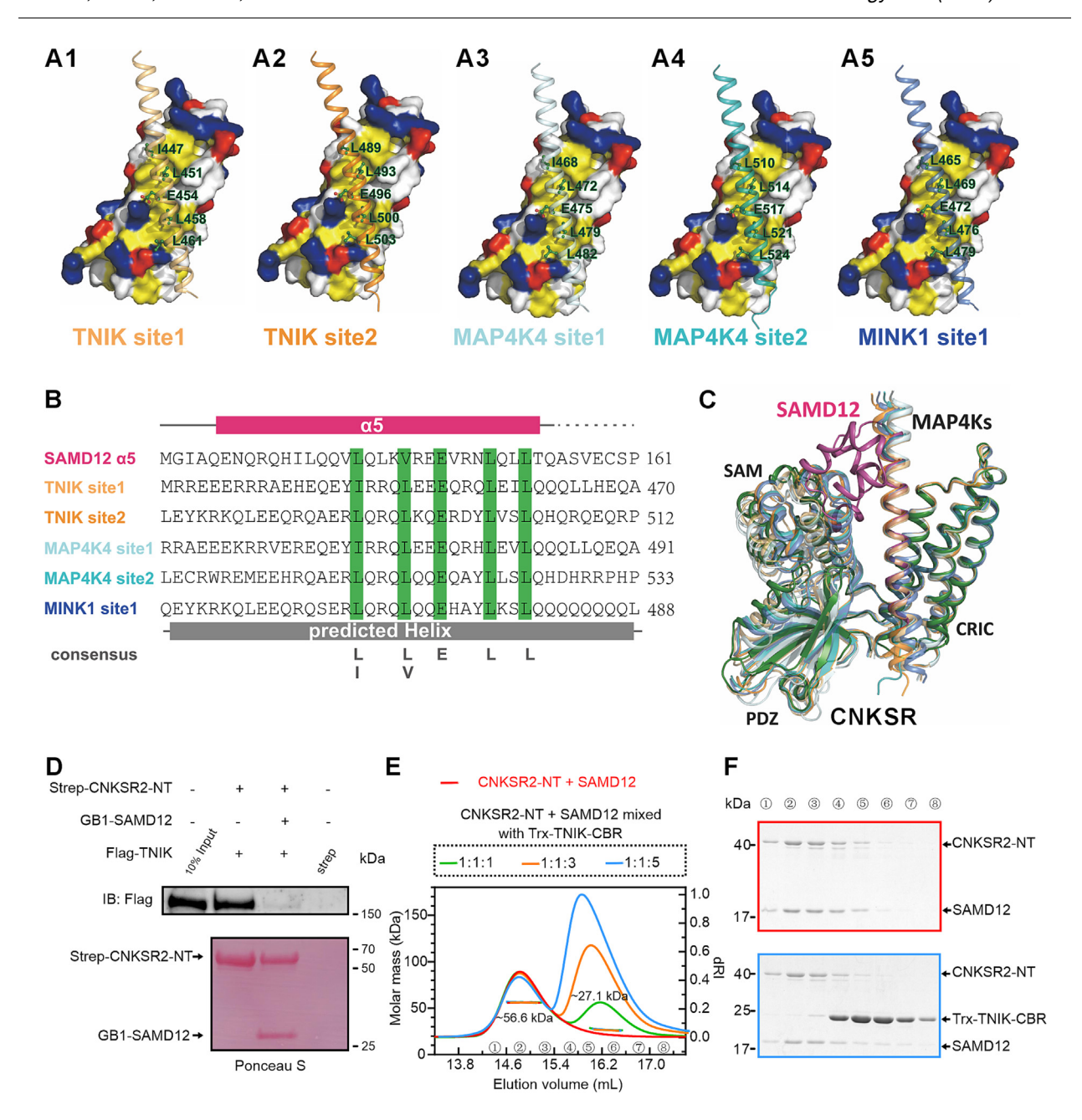


Figure 4. SAMD12 quantitatively titrates CNKSR2 to dissociate the CNKSR2/TNIK complex. (A) Combined surface and ribbon-stick representation showing the predicted interface between CNKSR2-CRIC and sites from MAP4Ks. Residues of the CRIC-binding motif are shown in green. (B) Sequence alignment of the CRIC-binding regions from the α5 helix of SAMD12, TNIK-site1/2, MAP4K4-site1/2, and MINK1-site1. The key residues for MAP4Ks' binding to CNKSRs are labeled in green. The consensus CRIC-binding motif L/I-X<sub>3</sub>-L/V-X<sub>2</sub>-E-X<sub>3</sub>-L-X<sub>2</sub>-L is shown beneath the alignment. (C) Superimposition of the CNKSR2-NT/SAMD12 complex crystal structure with the predicted structures of CNKSR2-NT in complex with TNIK-site1/2 (orange), MAP4K4-site1/2 (cyan) and MINK1-site1 (blue). (D) Pull-down-based competition assay showing that purified GB1-tagged SAMD12 potently disrupts the CNKSR2/TNIK interaction. (E) SEC-MALS analysis of a CNKSR2-NT/SAMD12 1:1 mixture (red line), a CNKSR2-NT/SAMD12/Trx-TNIK-CBR 1:1:3 mixture (orange line), and a CNKSR2-NT/SAMD12/Trx-TNIK-CBR 1:1:5 mixture (blue line). Measured molecular weights are indicated beneath the peaks. (F) SDS-PAGE with Coomassie blue staining showing the protein composition of the elution peak of the CNKSR2-NT/SAMD12/Trx-TNIK-CBR 1:1:5 mixture shown in red in panel (E), and the elution peak of the CNKSR2-NT/SAMD12/Trx-TNIK-CBR 1:1:5 mixture shown in blue in panel (E).

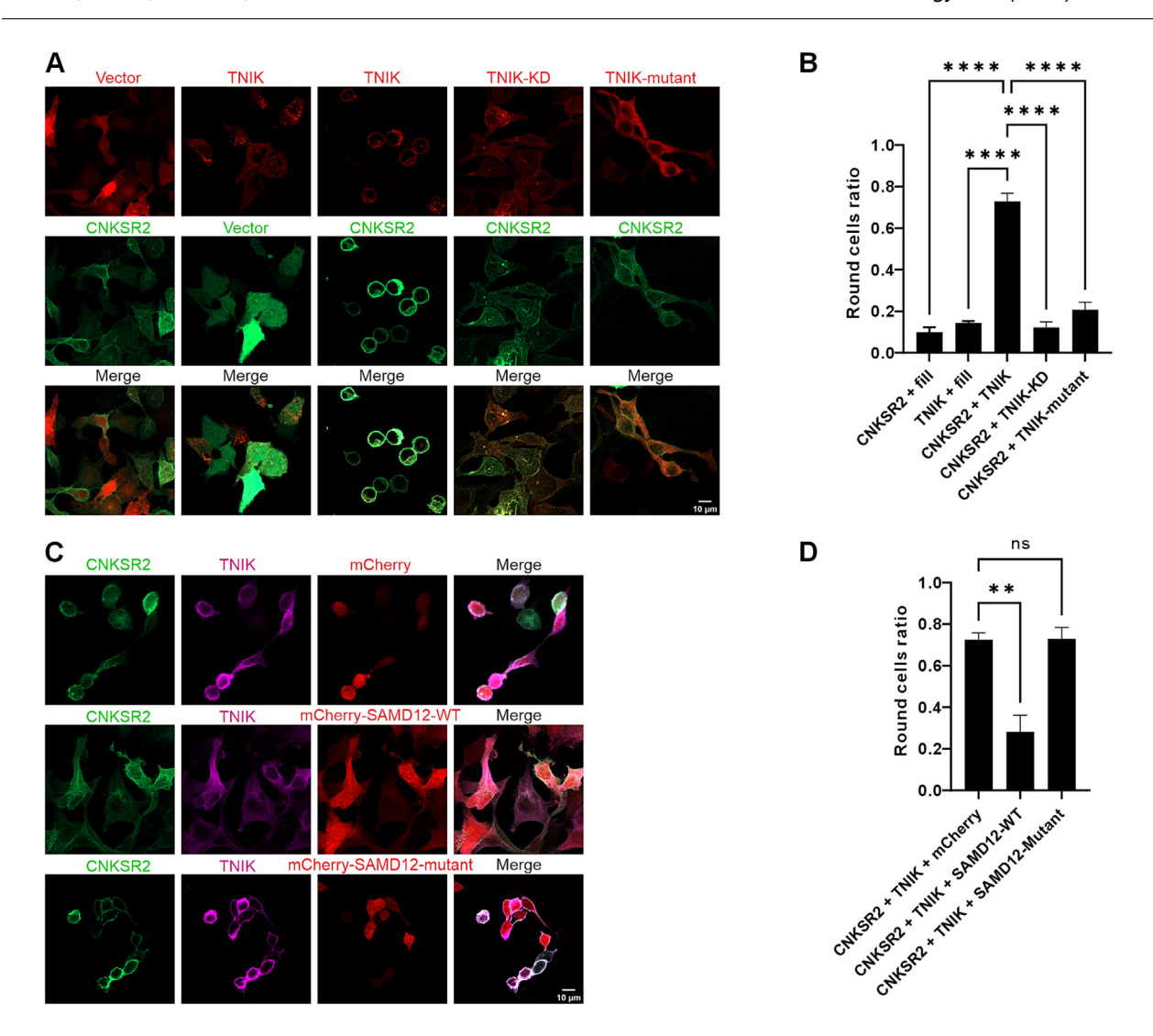


Figure 5. Membrane association-coupled activation of TNIK through CNKSR2 can be inhibited by SAMD12. (A) Cell rounding effects were observed when TNIK was recruited to plasma membrane by CNKSR2. Representative images of GFP-CNKSR2 co-expressed with the empty vector (mCherry), mCherry-TNIK, mCherry-TNIK-KD (TNIK-K54R, a kinase dead mutant) or mCherry-TNIK-mutant (deficient in binding to CNKSR2) in HEK293T cells. As a control, mCherry-TNIK co-expressed with GFP in HEK293T cells is also shown. Scale bar, 10  $\mu$ m. (B) Quantification of the ratio of round cells in each group as shown in panel (A). Data are represented as mean  $\pm$  SEM, from three independent experiments, n > 300. One-way ANOVA with Dunnett's multiple comparison test. ns, not significant; \*\*\*\*p < 0.0001. (C) SAMD12 inhibits the TNIK-induced cell rounding. Representative images showing HEK293T cells transfected with mCherry, mCherry-SAMD12-WT or mCherry-SAMD12-mutant deficient in binding to CNKSR2 with co-expression of GFP-CNKSR2 and Flag-TNIK. Anti-Flag was used to mark TNIK. Scale bar, 10  $\mu$ m. (D) Statistical results showing the ratio of round cells in panel (C). Data are represented as mean  $\pm$  SEM, from three independent experiments, n > 300. One-way ANOVA with Dunnett's multiple comparison test. ns, not significant; \*\*p < 0.001; \*\*\*\*\*p < 0.0001.

deficient TNIK-mutant is a valuable tool for studying the function of the CNKSR2/TNIK complex in heterologous cells described below.

### SAMD12 quantitatively titrates CNKSR2 to dissociate the CNKSR2/TNIK complex

Based on the interaction analysis between TNIK and CNKSR2 supported with the Alphafold3-based binding prediction, we can confidently

identify that MAP4K4 contains two CNKSR2 binding sites and MINK1 has one CNKSR2 binding site in each of their helical segment (Figures S3A and S3B). All these peptides bind to the CNK CRIC domain with a highly similar mode (Figure 4A and B). Combining the sequence alignment analysis in Figure 4B, a consensus CRIC-binding motif can be derived: L/I-X<sub>3</sub>-L/V-X<sub>2</sub>-E-X<sub>3</sub>-L-X<sub>2</sub>-L, where "X" denotes any residue, except for the helix disrupting residues such as

proline or glycine, and the subscript indicates the number of residues at this position (Figures 4B and 2D).

Aligning the solved CNKSR2-NT/SAMD12-SAM complex structure with the predicted structures of CNKSR2-NT in complex with CRIC-binding motifs from MAP4K4, TNIK and MINK1 (or MAP4K4/6/7 following the MAP4K family classification) revealed that the CBR of MAP4Ks and the α5 helix of SAMD12 use the same mode to interact **CNKSR2-CRIC** domain (Figure indicating that the binding of SAMD12 and MAP4Ks to CNKSRs are mutually exclusive. Since SAMD12 binds to CNKSRs with much higher affinities than MAP4Ks (low nM Kd vs subμM Kd; Figures 1D and 3K), SAMD12 would be able to effectively disrupt the interaction between CNKSRs and MAP4Ks in a dose-dependent manner. Indeed, StrepII-tagged CNKSR2-NT could robustly pull-down Flag-tagged full-length TNIK in a pull-down assay (Figure 4D, lane 2). Addition of purified SAMD12 protein into the mixture completely abrogated interaction between CNKSR2-NT and TNIK (Figure 4D, lane 3). We further showed by SEC-MALS analysis that in the presence stoichiometric amount of SAMD12 (i.e., SAMD12 and CNKSR2-NT were mixed in a 1:1 molar ratio), no TNIK-CBR could form complex with CNKSR2

even when up to a fivefold excess of TNIK-CBR was included in the mixtures (Figure 4E and F). These results imply that SAMD12 has a capacity to quantitatively displace MAP4Ks from the CNKSR scaffold proteins (i.e., formation of the MAP4K/CNKSR complexes in cells are extremely sensitive to the expression level of SAMD12).

### SAMD12 inhibits CNKSR2-mediated TNIK membrane association and activation

MAP4Ks play important roles in a variety of tissues and cells, but with poorly understood mechanisms. It has been reported that overexpression of wild type TNIK, but not the kinase-dead mutant of TNIK in heterologous cells results in disruption of F-actin, causing cell rounding. It has also been reported that Msn, an ortholog of TNIK/MAP4K4/MINK1 in drosophila, is activated upon associating with plasma membranes. Thus, it appears that recruitment of TNIK to the plasma membrane could activate TNIK's kinase activity, causing F-actin destabilization and consequent cell rounding.

Although also localized at other compartments,<sup>61</sup> CNKSR2 shows prominent association with the plasma membrane in neurons or heterologous cells, as demonstrated by the result in this study (Figure 5A and C) and from a previous study.<sup>62</sup>

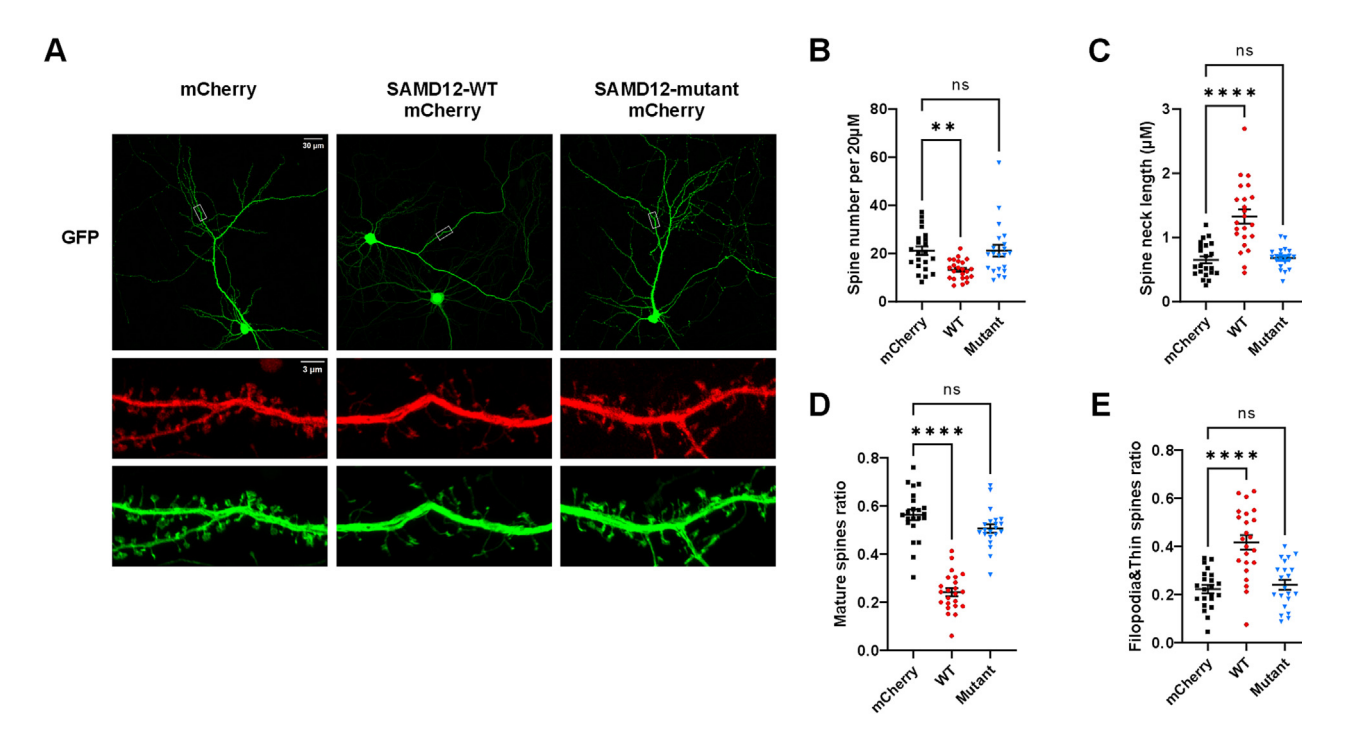


Figure 6. Perturbing the TNIK/CNSKR2 interaction in neurons leads to spine development defects. (A) Representative images showing dendritic spines in hippocampal neurons expressing GFP with mCherry, mCherry-SAMD12-WT or mCherry-SAMD12-mutant. The cultured neurons were transfected with indicated plasmids at DIV18 and fixed at DIV21 for imaging. (B-D) Quantification of the imaging data from 21 to 23 neurons from three independent batches of cultures. Data are represented as mean ± SEM. ns, not significant; \*\*p < 0.01; \*\*\*\*p < 0.0001, One-way ANOVA with Dunnett's multiple comparison test. Spines with mushroom heads were counted as mature spines.

When expressed alone in HEK293T cells, TNIK is either diffused or with some perinuclear or cell periphery punctate distributions and expressed cells are spread (Figure 5A and B). When TNIK and CNKSR2 were co-expressed, most cells became rounded with both TNIK and CNKSR2 highly enriched on the plasma membranes (Figure 5A and B). In sharp contrast, co-expression of the TNIK-mutant, which does not bind to CNKSR2 (Figure 3L), with CNKSR2 did not result in cell rounding and the expressed TNIK-mutant was diffused throughout the cytoplasm (Figure 5A and B). In addition, co-expression of the kinase-dead form of TNIK (TNIK-KD, TNIK with a lysine to arginine mutation in the kinase domain, K54R) with CNKSR2 also cannot cause cell rounding, although the expressed TNIK-KD was recruited to the plasma membrane by CNKSR2 (Figure 5A and B). These observations confirm that CNKSR2mediated TNIK membrane association and TNIK kinase activity are critical for TNIK-induced cell rounding.

As expected, SAMD12 could be recruited to plasma membranes by CNKSR2, overexpressed SAMD12 alone was diffused in cvtosol (Figure S3H). Upon co-expressing mCherry tagged SAMD12-WT with CNKSR2 and TNIK, the cell rounding phenotype was largely inhibited (Figure 5C and D), presumably due to the release of TNIK from CNKSR2 by SAMD12 4D and E). Consistent with interpretation, co-expression of mCherry or a mCherry tagged SAMD12-mutant (SAMD12 containing R113E, V142Q and L149Q triple point mutations, deficient in binding to CNKs) does not influence the cell rounding caused by CNKSR2mediated TNIK plasma membrane localization (Figure 5C and D).

### Perturbing the TNIK/CNKSR2 interaction in neurons causes synapse development defects

Genetic studies showed that deficiencies in CNKSR2 or TNIK cause overlapped defective neurodevelopmental phenotypes, likely because CNKSR2 can directly interact with TNIK and thereby regulate TNIK's activity as revealed in this study. Our study also suggests that SAMD12 can directly regulate TNIK's association with CNKSR2 and thereby modulate TNIK's activity in neurons. Totally fitting with this hypothesis, expression of mCherry-SAMD12 in cultured rat hippocampal neurons led to significant reductions in spine density (Figure 6A and B) and mature spines ratio (Figure 6D), with an accompanying increase of immature spines (Figure 6C and E). In sharp contrast, expression of mCherry or mCherry-tagged SAMD12-mutant defective in CNKSR2 binding had no impact on the spine development of neurons (Figure 6). Thus, using the cultured rat hippocampal neurons as the model, we have demonstrated that the interaction between CNKSR2 and TNIK, which

can be effectively regulated by the expression level of SAMD12, is important for synapse formation in neurons.

#### Discussion

#### SAMD12 and TNIK's function in neuron/ synapse and implications in neuronal development

TNIK and CNKSR2 not only interact with each other but also orchestrate distinct sets of synaptic protein complexes. <sup>15,65,66</sup> TNIK plays pivotal roles in postsynaptic pathways and is essential for normal cognitive function. For example, TNIK interacts with DISC1, a known risk factor for psychiatric diseases, to modulate synapse composition and functionality. <sup>67</sup> NMDAR and metabotropic receptors bidirectionally regulate the phosphorylation of TNIK, which is indispensable for AMPA receptor expression and synaptic function. <sup>21</sup> Given TNIK's involvement in multiple synaptic processes, it is imperative that its activity should be tightly controlled under varying synaptic conditions and at specific subcellular regions to ensure normal brain function.

The kinase activity and functional dynamics of TNIK are coupled with its subcellular localizations. For example, TNIK is activated to phosphorylate TCF4 when recruited into nucleus in a β-catenindependent manner. 7,8 In this study, we revealed that TNIK's activity is modulated by its membrane association through CNKSR2's recruitment. This mode of activation possibly stems from promoting the proximity of the kinase to effectors and activators on membranes, as supported by the finding that plasma membrane-enriched Rap2<sup>68</sup> could promote TNIK-induced cell rounding.<sup>2</sup> Correspondingly, SAMD12 via effectively competing TNIK from binding to CNKSR2 can potently inhibit TNIK's activity without directly targeting its kinase domain. Thus, the results presented in this study provide a possible molecular explanation why mutations of CNKSR2. TNIK and SAMD12 can result in overlapping neurodevelopmental phenotypes in patients.

Studies in postmortem brains of FAME patients suggest that SAMD12 transcription may terminate at the site of the repeat expansion, causing a slight but significant reduction in SAMD12 protein expression, 50 which should cause over activation of TNIK. It would be of considerable interest to explore in the future how the pentanucleotide repeat expansion in SAMD12 affects its expression level and the consequent impact on the TNIK activity in FAME patients or in animal models. At present, little is known about the molecular mechanism of SAMD12, except for human genetic studies pointing to roles of SAMD12 in neuronal development and neurodevelopmental disorders. 50,69-71 Our biochemical studies suggest a possible mechanism by which SAMD12 can effectively modulate the CNK-TNIK interaction. Our cell biology experiments further indicate that changes in the level of SAMD12

can alter TNIK activity in heterologous cells and in neurons. Therefore, we propose a model that the level change of SAMD12 under physiological or pathophysiological conditions can modulate the CNKSR2/TNIK interaction. Such a model should certainly be tested in future studies.

TNIK has been implicated in the pathophysiology of epilepsy. Notably, the expression of TNIK is significantly reduced in both epilepsy model rats and in patients with temporal lobe epilepsy. The inhibition of TNIK kinase activity by small molecule inhibitors has been shown to suppress epilepsy. Rap2 is a small GTPase act at the upstream of TNIK. Interestingly, Rapgef2, the guanine nucleotide exchange factor or activator for Rap2, is also a known FAME gene. In addition, the upstream of Rapgef2/Rap2, semaphorin and its plexin receptor are both linked to epilepsy pathology. It is plausible that these synaptic proteins may converge on a pathway that contributes to the pathophysiology of FAME, another topic worthy of future studies.

### A general model of SAMD12-tuned MAP4K activity regulation

TNIK and CNKSR2 are present in multiple subcellular compartments, including synapses. The present study is designed to explore the synaptic functionality of their interaction and to delineate its molecular relationship with SAMD12. It is important to note that this regulatory framework does not preclude its potential applicability in non-synaptic systems.

MAP4K4, TNIK, MINK1 are Misshapen family kinases widely expressed in neurons and nonneuronal cells and they share highly similar and sequence/structure have redundant functions.<sup>25</sup> Our data indicate that they interact with the CNKSR family proteins (CNKSR1, CNKSR2 and CNKSR3) using a similar binding mode. Although CNKSR2 is predominantly expressed in the nervous system, CNKSR1 and CNKSR3 are expressed across various tissues (Human Protein Atlas, https://www.proteinatlas.org). Thus, the CNKSR2 binding-mediated activation mechanism revealed here may be generally applicable to CNKSR-mediated activation of all three MAP4Ks. Similarly, both SAMD12 and SAMD10 can potently bind to CNKSRs and thus tune the three MAP4Ks activities in cells from various tissues. Given that the three MAP4Ks are closely associated with various human diseases including but not limited to neurodevelopmental disorders,<sup>73</sup> neurodegenerations,<sup>74</sup> various cancers,<sup>28,75</sup> immune disorders,<sup>76,77</sup> metabolic diseases,<sup>5</sup> and cardiovascular diseases. 78 the findings described in the current study will have general implications for understanding mechanisms underlying these diseases and for developing therapeutic strategies against these diseases.

#### Methods

#### Constructs and protein expression

Genes encoding various lengths of mouse CNKSR1 (NP 001074516; residues), 700 CNKSR2 (NP 808419; 1,032 residues), CNKSR3 residues), (NP\_766134; 555 SAMD10 residues), (NP\_766264; 202 SAMD12 (NP\_796199; 161 residues) and human TNIK (NP\_055843; 1,360 residues) were amplified by PCR and cloned into home-modified vectors containing an N-terminal Trx-His6/Trx-3xStrepII-Hise/GB1-Hise tag followed by an HRV-3C protease recognition site. Construct sequences confirmed by DNA sequencing. were Recombinant proteins were expressed in BL21codonplus Escherichia coli cells in LB medium to a OD<sub>600</sub> of 0.6-0.8 at 37 °C and then adding 0.3 mM IPTG (final concentration) to induce protein expression at 16 °C for about 20 h. The Nterminal Hise-tagged proteins were purified using Ni<sup>2+</sup>-nitrilotriacetic acid agarose (Cytiva; 17531803), followed by a step of size-exclusion chromatography (Cytiva; HiLoad 26/600 Superdex 200 pg column or HiLoad 26/600 Superdex 75 pg column) with the elution buffer containing 50 mM Tris-HCl pH 7.8, 100 mM NaCl, 1 mM EDTA and 1 mM DTT. When needed, recombinant protein tags were cleaved by HRV-3C protease at 4 °C for about 16 h and then removed by another step of size-exclusion chromatography. heterologous cell or neuronal expressions, the fulllength CNKSR2, TNIK, MINK1, MAP4K4 and SAMD12 genes, either WT or mutants, were cloned into pCMV-EGFP, pCMV-mCherry, pCMV-Flag or pCAG-mCherry vectors as described.

#### Isothermal titration calorimetry (ITC) assay

ITC measurements were carried out on MicroCal VP-ITC or ITC-200 or PEAQ-ITC calorimeters (Malvern Panalytical) at 25 °C or 16 °C. Titration buffer contained 50 mM Tris-HCl pH 7.8, 100 mM NaCl, 1 mM EDTA and 1 mM DTT. All protein solutions were degassed before loading to the injection syringe or the cell. Each titration point was performed by injecting a 10  $\mu l$  (for VP-ITC) or 2.5uL (for ITC200) or 2uL (for PEAQ-ITC) aliquot of a protein sample (200–400  $\mu M$ ) from the injection syringe into the cell containing another reactant (20–40  $\mu M$ ) with time intervals of 120 or 150 s. The titration data were analyzed by the Origin software from Microcal and fitted with the one-site binding model.

### Size-exclusion chromatography coupled with multi-angle light scattering (SEC-MALS) assay

SEC-MALS analysis was performed on a fast protein liquid chromatography (FPLC) system

(Cytiva) coupled with a static light-scattering detector (miniDAWN; Wyatt) and a differential refractive index (dRl) detector (Optilab; Wyatt). Protein samples (100  $\mu$ L) were loaded to a Superdex 200 Increase 10/300 GL column (Cytiva) pre-equilibrated with an assay buffer containing 50 mM Tris-HCl pH 7.8, 100 mM NaCl, 1 mM EDTA and 1 mM DTT on an AKTA FPLC system (Cytiva). Data were analyzed with Astra 8 (Wyatt).

### Affinity purification coupled with mass spectrometry (AP-MS)

C57BL/6J mice brain tissue were obtained in accordance with the ethical review of the laboratory animal welfare at the Shenzhen Bay Laboratory. The fresh brain tissue immediately homogenized in 50 mM HEPES pH 7.2, 600 mM NaCl, 15% glycerol, 0.1% Triton-X100. 20 mM CHAPS, 1 mM EDTA, 1 mM EGTA, 1 mM DTT, and a protease inhibitor cocktail (Cat. No. P8340, Sigma-Aldrich) using a tissue homogenizer for ~20 S. The homogenates were then subjected to centrifugation at 90,000g for 40 min using an Ultracentrifuge (Optima XPN 100, Beckman Coulter). The supernatant was collected and dialyzed in 20 mM HEPES pH 7.2, 200 mM NaCl, 5% glycerol, 1 mM EDTA, 1 mM EGTA, and 1 mM DTT, followed by another round of ultracentrifugation at 100,000g for 40 min. The protein concentration in the supernatant was determined using the Bradford assay.

For the affinity purification, the purified bait protein (StrepII-tagged CNK-NT protein) was conjugated to the Strep-Tactin Sepharose beads (Cytiva) through their Strepll tags. Brain lysate prepared in the previous step (1 ml for each sample) was precleared with Strep-Tactin beads and then mixed with the bait protein conjugated beads (20 µL dry volume for 1 ml lysate), and incubated for 15 min, then centrifuged at 1000a for 1 min. The pellets containing the beads was washed three times with the binding buffer to remove unbound proteins and then applied to SDS-PAGE. The SDS-PAGE gel was stained by Coomassie brilliant blue G-250 and protein bands were dissected for protein identification by Mass spectrometry by OmicSolution Ltd., Shanghai, China.

#### Crystallography

For screening protein crystals of the CNKSR2-NT/SAMD12-SAM complex, a construct of GB1 tagged SAMD12 (aa 78–161) was fused to the N-terminus of CNKSR2 (aa 1–314) by a flexible linker containing the TEV recognition sequence (-ENLYFQGGSGSG-) to generate a fusion protein. The purified fusion protein was subjected to HRV-3C protease digestion and TEV protease

diaestion. followed bv size-exclusion chromatography to remove the tags and get a 1:1 ratio protein complex in a buffer containing 50 mM Tris-HCl pH 7.8, 100 mM NaCl, 1 mM EDTA and 1 mM DTT. Crystals of this protein complex was generated by sitting drop vapor diffusion methods at 16 °C, in the reservoir buffer containing 0.1 M HEPES pH 7.5, 10% w/v Polyethylene glycol 8,000 and 8% v/v Ethylene glycol. Crystals were cryoprotected with 25% (v/v) glycerol and flash-cooled to 100 K. X-ray diffraction data were collected at the BL19U1 beamline of the Shanghai Synchrotron Radiation Facility (SSRF). Data were processed and scaled using HKL3000.<sup>79</sup> Structures were solved by molecular replacement using PHASER,80 using the structures of the drosophila CNK/HYP complex (PDB: 3BS5) and mouse MUPP1 PDZ4 (PDB: 4XH7) as the searching model. Further model building and refinement were completed iteratively using COOT<sup>81</sup> and Phenix.<sup>82</sup> The final model was validated by MolProbity<sup>83</sup> and statistics are summarized in Table S1. All structure figures were prepared by PyMOL (https://www.pymol.org).

#### **Pull-down assay**

For pull-down assays, the full-length Flag-tagged TNIK/MINK1/MAP4K4 or truncated Flag-TNIK constructs were expressed in HEK293T cells. 24 h after transfection, cells were lysed in the ice-cold cell lysis buffer containing 20 mM HEPES pH 7.0, 150 mM NaCl, 1 mM EDTA, 1% NP-40, Phosphatase inhibitor cocktail (Millipore; 524629) Protease inhibitor (MedChemExpress; HY-K0010) for 1 h at 4 °C. After centrifuging at 14,000 rpm for 10 min at 4  $^{\circ}$ C, supernatants were collected for pull-down assays. In each reaction, the supernatant was incubated with 0.5 µM (final concentration) purified Trx-StrepII-tagged CNKSR2-Nter or Trx-StrepII tag for 1 h at 4 °C, then incubated for another 30 min at 4 °C with 15 µl StrepTactin agarose beads (AlpalifeBio; KTSM1350). competition group, 1 µM (final concentration) purified GB1-SAMD12 protein was added together with Trx-StrepII-tagged CNKSR2-Nter protein. After extensive washing, the captured proteins were eluted with SDS-PAGE and detected by western blot using anti-Flag antibody (1:5,000; Sigma-Aldrich; F1804).

#### **HEK293T cell culture and imaging**

HEK293T cells (originated from ATCC) were cultured in DMEM (HyClone; SH30243.01) supplemented with 10% FBS (TOCYTO; UT83998) at 37 °C with 5% CO<sub>2</sub>. Cells were seeded onto dishes at a density of 90,000/well on 12-well plates (Greiner; 665180). 20 h after plating, the cells were transfected with

corresponding plasmids with Polyethylenimine (PEI) Max (Polysciences; 24765-100). The transfected cells were cultured for 20 h before fixation.

For immunocytochemistry, cells were permeabilized with 0.2% Triton X-100 in PBS for . 10 min, and then blocked with 3% Normal Donkey Serum (NDS) in PBST (0.1% Tween-20 in PBS) for 1 h. Then the cells were incubated with mouse anti-Flag antibody (1:1,000; Sigma-Aldrich; F1804) in blocking buffer at 4 °C overnight. On the next day, cells were rinsed three times (10 min each) with PBST and stained with Alexa Fluor 647 labeled anti-mouse secondary antibody (1:500; Invitrogen; A31571) for 1 h at room temperature, then washed and mounted with 14 µL Fluoro-gel (Electron Microscopy Sciences: 17985-11) before imaging. All HEK293T cell culture images were acquired with a Zeiss LSM 980 laser-scanning confocal microscope. Images were captured using a 20× objective for quantification and a 63× oil objective for zoom-in visualization. The images were then analyzed with ImageJ software. All round cells were manually counted. experiments were conducted in a double-blinded mode and data were collected from three batches of independent experiments. Over 300 cells from each group were assayed for the cell rounding quantification. Data were checked for their normal distribution and expressed as mean ± SEM, Oneway ANOVA with Dunnett's multiple comparison test were used for analyze the significance.

### Primary hippocampal neuron culture, transfection and imaging

Primary hippocampal neuron cultures were prepared from E19.5 SD rat (Charles River; G20240306) hippocampi. Digested cells were seeded on coverslips coated by Poly-D-lysine (Sigma-Aldrich; P7280) on 12-well plates (Greiner; 665180). Cultures were maintained for 21 days in vitro (DIV) in Neurobasal media (Gibco: 21103049) supplemented with GlutaMAX (Gibco: 35050061) and B-27 (Gibco; 17504044). Cells were co-transfected at DIV18 with 2 μg DNA plasmids per well using Lipofectamine 2000 reagent (Invitrogen; 11668019). Cells were fixed at DIV21 with 4% (vol/vol) paraformaldehyde (diluted in PBS) containing 4% (wt/vol) sucrose for 20 min at room temperature and then mounted on slides for imaging. All images were acquired with a Zeiss LSM 980 laser-scanning confocal microscope with a 40 × 0.6 oil-immersion objective. Transfected pyramidal neurons were chosen randomly for quantification from three independent batches of cultures. For detailed spine visualization, an additional 4× zoom factor was applied. The secondary branches ( $\sim$ 60  $\mu$ M in length) from the apical dendrites were imaged and analyzed from an individual neuron. Each image

was collected as a z series maximum projection with 0.7- $\mu$ M (for neuron) or 0.4- $\mu$ M (for branch) depth intervals and projected to a 2D image using a maximum intensity operation. Spine density and spine neck length were measured with ImageJ.

#### **Author contributions**

K. Chen and M. Zhang conceived the idea and designed the experiments; W. Pan performed all biochemical experiments and cell biology experiments with helps from S. Chen, J. Li, and Y. Wang; Z. Lin solved the crystal structure of the complex; W. Pan, K. Chen, and M. Zhang wrote the manuscript with input from other authors. K. Chen and M. Zhang supervised the research. M. Zhang coordinated the project.

### CRediT authorship contribution statement

Wen Pan: Investigation. Zhijie Lin: Investigation. Shiwen Chen: Investigation. Jiahui Li: Investigation. Yu Wang: Investigation. Keyu Chen: Writing – original draft, Supervision, Investigation. Mingjie Zhang: Writing – review & editing, Writing – original draft, Supervision, Resources, Formal analysis, Conceptualization.

#### **DATA AVAILABILITY**

Data will be made available on request.

#### **DECLARATION OF COMPETING INTEREST**

The authors declare that they have no known competing financial interests or personal relationships that could have appeared to influence the work reported in this paper.

#### **Acknowledgement**

We thank the BL19U1 beamline at National Facility for Protein Science Shanghai (NFPS) for X-ray beam time. This work was funded by Key-Area Development Program of Research and Guangdong Province (2023B0303010001), the Major Program of Shenzhen Bay Laboratory (S201101002), the National Natural Science Foundation of China (82188101), Shenzhen Talent Program (KQTD20210811090115021), Shenzhen Science and Technology Program (ZDSYS20220402111000001), Shenzhen Technology Basic Research Science and Program (JCYJ20220818100215033), Guangdong Innovative and Entrepreneurial Research Team Program (2021ZT09Y104) and Shenzhen Medical Research Fund (B2302039) to MZ.

#### Appendix A. Supplementary material

Supplementary material to this article can be found online at https://doi.org/10.1016/j.jmb.2025. 169034.

Received 23 December 2024; Accepted 19 February 2025; Available online 24 February 2025

> Keywords: CNKSR2; neurodevelopmental disorders; SAMD12; TNIK; MAP4K

#### References

- Fu, C.A., Shen, M., Huang, B.C., Lasaga, J., Payan, D.G., Luo, Y., (1999). TNIK, a novel member of the germinal center kinase family that activates the c-Jun N-terminal kinase pathway and regulates the cytoskeleton. *J. Biol. Chem.* 274, 30729–30737.
- Taira, K., Umikawa, M., Takei, K., Myagmar, B.E., Shinzato, M., Machida, N., et al., (2004). The Traf2- and Nck-interacting kinase as a putative effector of Rap2 to regulate actin cytoskeleton. *J. Biol. Chem.* 279, 49488– 49496.
- Chon, H.J., Lee, Y., Bae, K.J., Byun, B.J., Kim, S.A., Kim, J., (2016). Traf2- and Nck-interacting kinase (TNIK) is involved in the anti-cancer mechanism of dovitinib in human multiple myeloma IM-9 cells. *Amino Acids* 48, 1591–1599.
- Kukimoto-Niino, M., Shirouzu, M., Yamada, T., (2022). Structural insight into TNIK inhibition. *Int. J. Mol. Sci.* 23
- Pham, T.C.P., Dollet, L., Ali, M.S., Raun, S.H., Moller, L.L. V., Jafari, A., et al., (2023). TNIK is a conserved regulator of glucose and lipid metabolism in obesity. Sci. Adv. 9, eadf7119.
- Wu, X., Zhang, Z., Qiu, Z., Wu, X., Chen, J., Liu, L., et al., (2024). TNIK in disease: from molecular insights to therapeutic prospects. *Apoptosis* 29, 1361–1376.
- Ewald, C.Y., Pulous, F.E., Lok, S.W.Y., Pun, F.W., Aliper, A., Ren, F., et al., (2024). TNIK's emerging role in cancer, metabolism, and age-related diseases. *Trends Pharmacol. Sci.* 45, 478–489.
- Mahmoudi, T., Li, V.S., Ng, S.S., Taouatas, N., Vries, R.G., Mohammed, S., et al., (2009). The kinase TNIK is an essential activator of Wnt target genes. *EMBO J.* 28, 3329– 3340.
- Nonaka, H., Takei, K., Umikawa, M., Oshiro, M., Kuninaka, K., Bayarjargal, M., et al., (2008). MINK is a Rap2 effector for phosphorylation of the postsynaptic scaffold protein TANC1. *Biochem. Biophys. Res. Commun.* 377, 573–578.
- Chen, X., Shibata, A.C., Hendi, A., Kurashina, M., Fortes, E., Weilinger, N.L., et al., (2018). Rap2 and TNIK control Plexin-dependent tiled synaptic innervation in C. elegans. *Flifa* 7
- Hussain, N.K., Hsin, H., Huganir, R.L., Sheng, M., (2010).
  MINK and TNIK differentially act on Rap2-mediated signal

- transduction to regulate neuronal structure and AMPA receptor function. *J. Neurosci.* **30**, 14786–14794.
- Kawabe, H., Neeb, A., Dimova, K., Young Jr., S.M., Takeda, M., Katsurabayashi, S., et al., (2010). Regulation of Rap2A by the ubiquitin ligase Nedd4-1 controls neurite development. *Neuron* 65, 358–372.
- Teuliere, J., Gally, C., Garriga, G., Labouesse, M., Georges-Labouesse, E., (2011). MIG-15 and ERM-1 promote growth cone directional migration in parallel to UNC-116 and WVE-1. Development 138, 4475–4485.
- Locke, C.J., Kautu, B.B., Berry, K.P., Lee, S.K., Caldwell, K.A., Caldwell, G.A., (2009). Pharmacogenetic analysis reveals a post-developmental role for Rac GTPases in Caenorhabditis elegans GABAergic neurotransmission. Genetics 183, 1357–1372.
- Burette, A.C., Phend, K.D., Burette, S., Lin, Q., Liang, M., Foltz, G., et al., (2015). Organization of TNIK in dendritic spines. J. Comp. Neurol. 523, 1913–1924.
- Jiang, J., Wilkinson, B., Flores, I., Hartel, N., Mihaylov, S. R., Clementel, V.A., et al., (2024). Mutations in the postsynaptic density signaling hub TNIK disrupt PSD signaling in human models of neurodevelopmental disorders. Front. Mol. Neurosci. 17, 1359154.
- Lin, T.B., Hsieh, M.C., Lai, C.Y., Cheng, J.K., Chau, Y.P., Ruan, T., et al., (2015). Fbxo3-dependent Fbxl2 ubiquitination mediates neuropathic allodynia through the TRAF2/TNIK/GluR1 cascade. *J. Neurosci.* 35, 16545– 16560.
- MacLaren, E.J., Charlesworth, P., Coba, M.P., Grant, S.G., (2011). Knockdown of mental disorder susceptibility genes disrupts neuronal network physiology in vitro. Mol. Cell. Neurosci. 47, 93–99.
- Zieger, H.L., Kunde, S.A., Rademacher, N., Schmerl, B., Shoichet, S.A., (2020). Disease-associated synaptic scaffold protein CNK2 modulates PSD size and influences localisation of the regulatory kinase TNIK. Sci. Rep. 10, 5709.
- Anazi, S., Shamseldin, H.E., AlNaqeb, D., Abouelhoda, M., Monies, D., Salih, M.A., et al., (2016). A null mutation in TNIK defines a novel locus for intellectual disability. *Hum. Genet.* 135, 773–778.
- Coba, M.P., Komiyama, N.H., Nithianantharajah, J., Kopanitsa, M.V., Indersmitten, T., Skene, N.G., et al., (2012). TNiK is required for postsynaptic and nuclear signaling pathways and cognitive function. *J. Neurosci.* 32, 13987–13999.
- Potkin, S.G., Turner, J.A., Guffanti, G., Lakatos, A., Fallon, J.H., Nguyen, D.D., et al., (2009). A genome-wide association study of schizophrenia using brain activation as a quantitative phenotype. Schizophr. Bull. 35, 96–108.
- lossifov, I., O'Roak, B.J., Sanders, S.J., Ronemus, M., Krumm, N., Levy, D., et al., (2014). The contribution of de novo coding mutations to autism spectrum disorder. *Nature* 515, 216–221.
- Genovese, G., Fromer, M., Stahl, E.A., Ruderfer, D.M., Chambert, K., Landén, M., et al., (2016). Increased burden of ultra-rare protein-altering variants among 4,877 individuals with schizophrenia. *Nature Neurosci.* 19, 1433–1441.
- Larhammar, M., Huntwork-Rodriguez, S., Rudhard, Y., Sengupta-Ghosh, A., Lewcock, J.W., (2017). The Ste20 family kinases MAP4K4, MINK1, and TNIK converge to regulate stress-induced JNK signaling in neurons. *J. Neurosci.* 37, 11074–11084.

- Huang, H., Han, Q., Zheng, H., Liu, M., Shi, S., Zhang, T., et al., (2021). MAP4K4 mediates the SOX6-induced autophagy and reduces the chemosensitivity of cervical cancer. *Cell Death Dis.* 13, 13.
- Singh, S.K., Roy, R., Kumar, S., Srivastava, P., Jha, S., Rana, B., et al., (2023). Molecular insights of MAP4K4 signaling in inflammatory and malignant diseases. *Cancers* (Basel) 15
- Yu, D.H., Zhang, X., Wang, H., Zhang, L., Chen, H., Hu, M., et al., (2014). The essential role of TNIK gene amplification in gastric cancer growth. *Oncogenesis*. 2, e89
- 29. Huang, X., Hao, C., Shen, X., Liu, X., Shan, Y., Zhang, Y., et al., (2013). Differences in the transcriptional profiles of human cumulus cells isolated from MI and MII oocytes of patients with polycystic ovary syndrome. *Reproduction* 145, 597–608.
- **30.** Yue, M., Luo, D.J., Yu, S.S., Liu, P., Zhou, Q., Hu, M.J., et al., (2016). Misshapen/NIK-related kinase (MINK1) is involved in platelet function, hemostasis, and thrombus formation. *Blood* **127**, 927–937.
- Ohtakara, K., Nishizawa, M., Izawa, I., Hata, Y., Matsushima, S., Taki, W., et al., (2002). Densin-180, a synaptic protein, links to PSD-95 through its direct interaction with MAGUIN-1. *Genes Cells* 7, 1149–1160.
- 32. Yao, I., Hata, Y., Ide, N., Hirao, K., Deguchi, M., Nishioka, H., et al., (1999). MAGUIN, a novel neuronal membrane-associated guanylate kinase-interacting protein. *J. Biol. Chem.* 274, 11889–11896.
- 33. Maruo, T., Mizutani, K., Miyata, M., Kuriu, T., Sakakibara, S., Takahashi, H., et al., (2023). s-Afadin binds to MAGUIN/Cnksr2 and regulates the localization of the AMPA receptor and glutamatergic synaptic response in hippocampal neurons. *J. Biol. Chem.* 299, 103040.
- 34. Ito, H., Nagata, K.I., (2022). Functions of CNKSR2 and its association with neurodevelopmental disorders. *Cells* 11
- Maisonneuve, P., Sahmi, M., Bergeron-Labrecque, F., Ma, X.I., Queguiner, J., Arseneault, G., et al., (2024). The CNK-HYP scaffolding complex promotes RAF activation by enhancing KSR-MEK interaction. *Nature Struct. Mol. Biol.* 31, 1028–1038.
- Lanigan, T.M., Liu, A., Huang, Y.Z., Mei, L., Margolis, B., Guan, K.L., (2003). Human homologue of Drosophila CNK interacts with Ras effector proteins Raf and Rlf. FASEB J. 17, 2048–2060.
- Lim, J., Ritt, D.A., Zhou, M., Morrison, D.K., (2014). The CNK2 scaffold interacts with vilse and modulates Rac cycling during spine morphogenesis in hippocampal neurons. *Curr. Biol.* 24, 786–792.
- 38. Ito, H., Morishita, R., Noda, M., Ishiguro, T., Nishikawa, M., Nagata, K.I., (2021). The synaptic scaffolding protein CNKSR2 interacts with CYTH2 to mediate hippocampal granule cell development. J. Biol. Chem. 297, 101427.
- Vaags, A.K., Bowdin, S., Smith, M.L., Gilbert-Dussardier, B., Brocke-Holmefjord, K.S., Sinopoli, K., et al., (2014). Absent CNKSR2 causes seizures and intellectual, attention, and language deficits. *Ann. Neurol.* 76, 758–764.
- Aypar, U., Wirrell, E.C., Hoppman, N.L., (2015). CNKSR2 deletions: a novel cause of X-linked intellectual disability and seizures. Am. J. Med. Genet. A 167, 1668–1670.
- 41. Higa, L.A., Wardley, J., Wardley, C., Singh, S., Foster, T., Shen, J.J., (2021). CNKSR2-related neurodevelopmental and epilepsy disorder: a cohort of 13 new families and literature review indicating a predominance of loss of

- function pathogenic variants. *BMC Med. Genomics* 14, 186.
- Damiano, J.A., Burgess, R., Kivity, S., Lerman-Sagie, T., Afawi, Z., Scheffer, I.E., et al., (2017). Frequency of CNKSR2 mutation in the X-linked epilepsy-aphasia spectrum. *Epilepsia* 58, e40–e43.
- Houge, G., Rasmussen, I.H., Hovland, R., (2012). Loss-offunction CNKSR2 mutation is a likely cause of nonsyndromic X-linked intellectual disability. *Mol. Syndromol.* 2, 60–63.
- Erata, E., Gao, Y., Purkey, A.M., Soderblom, E.J., McNamara, J.O., Soderling, S.H., (2021). Cnksr2 loss in mice leads to increased neural activity and behavioral phenotypes of epilepsy-aphasia syndrome. *J. Neurosci.* 41, 9633–9649.
- Therrien, M., Wong, A.M., Rubin, G.M., (1998). CNK, a RAF-binding multidomain protein required for RAS signaling. Cell 95, 343–353.
- Therrien, M., Wong, A.M., Kwan, E., Rubin, G.M., (1999). Functional analysis of CNK in RAS signaling. PNAS 96, 13259–13263.
- Douziech, M., Roy, F., Laberge, G., Lefrancois, M., Armengod, A.V., Therrien, M., (2003). Bimodal regulation of RAF by CNK in Drosophila. *EMBO J.* 22, 5068–5078.
- 48. Rocheleau, C.E., Rönnlund, A., Tuck, S., Sundaram, M.V. *Caenorhabditis elegans* CNK-1 promotes Raf activation but is not essential for Ras/Raf signaling.
- Cuccurullo, C., Striano, P.A.-O., Coppola, A.A.-O. Familial adult myoclonus epilepsy: a non-coding repeat expansion disorder of cerebellar-thalamic-cortical loop. LID – 10. 3390/cells12121617 [doi] LID – 1617.
- Ishiura, H., Doi, K., Mitsui, J., Yoshimura, J., Matsukawa, M.K., Fujiyama, A., et al., (2018). Expansions of intronic TTTCA and TTTTA repeats in benign adult familial myoclonic epilepsy. *Nature Genet.* 50, 581–590.
- Florian, R.T., Kraft, F., Leitao, E., Kaya, S., Klebe, S., Magnin, E., et al., (2019). Unstable TTTTA/TTTCA expansions in MARCH6 are associated with familial adult myoclonic epilepsy type 3. Nature Commun. 10, 4919.
- Yeetong, P., Pongpanich, M., Srichomthong, C., Assawapitaksakul, A., Shotelersuk, V., Tantirukdham, N., et al., (2019). TTTCA repeat insertions in an intron of YEATS2 in benign adult familial myoclonic epilepsy type 4. *Brain* 142, 3360–3366.
- Corbett, M.A., Kroes, T., Veneziano, L., Bennett, M.F., Florian, R., Schneider, A.L., et al., (2019). Intronic ATTTC repeat expansions in STARD7 in familial adult myoclonic epilepsy linked to chromosome 2. *Nature Commun.* 10, 4920.
- Serwe, G., Kachaner, D., Gagnon, J., Plutoni, C., Lajoie, D., Durame, E., et al., (2023). CNK2 promotes cancer cell motility by mediating ARF6 activation downstream of AXL signalling. *Nature Commun.* 14, 3560.
- Rajakulendran, T., Sahmi, M., Kurinov, I., Tyers, M., Therrien, M., Sicheri, F., (2008). CNK and HYP form a discrete dimer by their SAM domains to mediate RAF kinase signaling. PNAS 105, 2836–2841.
- Douziech, M., Sahmi, M., Laberge, G., Therrien, M., (2006). A KSR/CNK complex mediated by HYP, a novel SAM domain-containing protein, regulates RAS-dependent RAF activation in Drosophila. *Genes Dev.* 20, 807–819.
- Lim, J., Zhou, M., Veenstra, T.D., Morrison, D.K., (2010).
  The CNK1 scaffold binds cytohesins and promotes insulin pathway signaling. *Genes Dev.* 24, 1496–1506.

- Wang, Y., Shang, Y., Li, J., Chen, W., Li, G., Wan, J., et al., (2018). Specific Eph receptor-cytoplasmic effector signaling mediated by SAM-SAM domain interactions. *Elife* 7
- Abramson, J., Adler, J., Dunger, J., Evans, R., Green, T., Pritzel, A., et al., (2024). Accurate structure prediction of biomolecular interactions with AlphaFold 3. Nature 630, 493–500.
- Kaneko, S., Chen, X., Lu, P., Yao, X., Wright, T.G., Rajurkar, M., et al., (2011). Smad inhibition by the Ste20 kinase Misshapen. PNAS 108, 11127–11132.
- Yin, L., Xu, Y., Mu, J., Leng, Y., Ma, L., Zheng, Y., et al., (2025). CNKSR2 interactome analysis indicates its association with the centrosome/microtubule system. Neural Regen. Res. 20, 2420–2432.
- Isakoff, S.J., Cardozo, T., Andreev, J., Li, Z., Ferguson, K. M., Abagyan, R., et al., (1998). Identification and analysis of PH domain-containing targets of phosphatidylinositol 3-kinase using a novel *in vivo* assay in yeast. *EMBO J.* 17, 5374–5387.
- 63. Hu, H., Haas, S.A., Chelly, J., Van Esch, H., Raynaud, M., de Brouwer, A.P., et al., (2016). X-exome sequencing of 405 unresolved families identifies seven novel intellectual disability genes. *Mol. Psychiatry* 21, 133–148.
- 64. Bonardi, C.M., Mignot, C., Serratosa, J.M., Giraldez, B.G., Moretti, R., Rudolf, G., et al., (2020). Expanding the clinical and EEG spectrum of CNKSR2-related encephalopathy with status epilepticus during slow sleep (ESES). Clin. Neurophysiol. 131, 1030–1039.
- Li, J., Zhang, W., Yang, H.A.-O., Howrigan, D.P., Wilkinson, B., Souaiaia, T., et al. Spatiotemporal profile of postsynaptic interactomes integrates components of complex brain disorders.
- 66. Jiang, J., Wilkinson, B., Flores, I., Hartel, N., Mihaylov, S. R., Clementel, V.A., et al. Mutations in the postsynaptic density signaling hub TNIK disrupt PSD signaling in human models of neurodevelopmental disorders.
- Wang, Q., Charych, E.I., Pulito, V.L., Lee, J.B., Graziane, N.M., Crozier, R.A., et al., (2011). The psychiatric disease risk factors DISC1 and TNIK interact to regulate synapse composition and function. *Mol. Psychiatry* 16, 1006–1023.
- 68. Ohba, Y., Mochizuki, N., Matsuo, K., Yamashita, S., Nakaya, M., Nakaya, M., Hashimoto, Y., Hamaguchi, M., et al. Rap2 as a slowly responding molecular switch in the Rap1 signaling cascade.
- 69. Chen, X.A.-O., Zhang, F., Shi, Y., Wang, H., Chen, M., Yang, D., et al. Origin and evolution of pentanucleotide repeat expansions at the familial cortical myoclonic tremor with epilepsy type1 SAMD12 locus. LID 10.1038/s41431-024-01586-y [doi].
- Yeetong, P., Chunharas, C., Pongpanich, M.A.-O., Bennett, M.F., Srichomthong, C., Pasutharnchat, N., et al. Founder effect of the TTTCA repeat insertions in SAMD12 causing BAFME1.

- Corbett, M.A.-O., Depienne, C.A.-O., Veneziano, L.A.-O., Klein, K.A.-O., Brancati, F., Guerrini, R., et al. Genetics of familial adult myoclonus epilepsy: From linkage studies to noncoding repeat expansions.
- Wang, M., Gu, Y., Li, Q., Feng, B., Lv, X., Zhang, H., et al., (2024). The Traf2 and NcK interacting kinase inhibitor NCB-0846 suppresses seizure activity involving the decrease of GRIA1. Genes Dis. 11, 100997.
- 73. Potkin, S.G., Turner, J., Guffanti, G., Lakatos, A., Fallon, J. H., Nguyen, D.D., Mathalon, D., et al. A genome-wide association study of schizophrenia using brain activation as a quantitative phenotype.
- 74. Yang, Y.M., Gupta, S., Kim, K.J., Powers, B.E., Cerqueira, A., Wainger, B.J., Ngo, H.D., et al. A small molecule screen in stem-cell-derived motor neurons identifies a kinase inhibitor as a candidate therapeutic for ALS.
- Gui, J., Yang, B., Wu, J., Zhou, X. Enormous influence of TNIK knockdown on intracellular signals and cell survival.
- Huang, H., Tang, Q., Chu, H., Jiang, J., Zhang, H., Hao, W., et al., (2014). MAP4K4 deletion inhibits proliferation and activation of CD4(+) T cell and promotes T regulatory cell generation in vitro. Cell. Immunol. 289, 15–20.
- Chuang, H.C., Sheu, W.H., Lin, Y.T., Tsai, C.Y., Yang, C. Y., Cheng, Y.J., et al., (2014). HGK/MAP4K4 deficiency induces TRAF2 stabilization and Th17 differentiation leading to insulin resistance. *Nature Commun.* 5, 4602.
- Fuller, S.J., Edmunds, N.S., McGuffin, L.J., Hardyman, M. A., Cull, J.J., Alharbi, H.O., et al., (2021). MAP4K4 expression in cardiomyocytes: multiple isoforms, multiple phosphorylations and interactions with striatins. *Biochem. J.* 478, 2121–2143.
- Minor, W., Cymborowski, M., Otwinowski, Z., Chruszcz, M., (2006). HKL-3000: the integration of data reduction and structure solution–from diffraction images to an initial model in minutes. *Acta Crystallogr. D Biol. Crystallogr.* 62, 859–866.
- McCoy, A., Grosse-Kunstleve, R.W., Adams, P.D., Winn, M.D., Storoni, L.C., Read, R.J., (2007). Phaser crystallographic software. *J. Appl. Crystallogr.* 40, 658– 674.
- Emsley, P., Lohkamp, B., Scott, W.G., Cowtan, K., (2010).
  Features and development of Coot. Acta Crystallogr. D Biol. Crystallogr. 66, 486–501.
- Adams, P.D., Afonine, P.V., Bunkoczi, G., Chen, V.B., Davis, I.W., Echols, N., et al., (2010). PHENIX: a comprehensive Python-based system for macromolecular structure solution. *Acta Crystallogr. D Biol. Crystallogr.* 66, 213–221.
- Chen, V.B., Arendall 3rd, W.B., Headd, J.J., Keedy, D.A., Immormino, R.M., Kapral, G.J., et al., (2010). MolProbity: all-atom structure validation for macromolecular crystallography. Acta Crystallogr. D Biol. Crystallogr. 66, 12–21.